



Politecnico  
di Bari

Repository Istituzionale dei Prodotti della Ricerca del Politecnico di Bari

An optimization procedure for Microgrid day-ahead operation in the presence of CHP facilities

This is a post print of the following article

*Original Citation:*

An optimization procedure for Microgrid day-ahead operation in the presence of CHP facilities / Aluisio, Benedetto; Dicorato, Maria; Forte, Giuseppe; Trovato, Michele Antonio. - In: SUSTAINABLE ENERGY, GRIDS AND NETWORKS. - ISSN 2352-4677. - 11:(2017), pp. 34-45. [10.1016/j.segan.2017.07.003]

*Availability:*

This version is available at <http://hdl.handle.net/11589/116944> since: 2022-06-07

*Published version*

DOI:10.1016/j.segan.2017.07.003

Publisher:

*Terms of use:*

(Article begins on next page)

# 1 **An optimization procedure for Microgrid day-ahead operation in the** 2 **presence of CHP facilities**

3 B. Aluisio<sup>a</sup>, M. Dicorato<sup>a</sup>, G. Forte<sup>a</sup>, M. Trovato<sup>a,\*</sup>

4 <sup>a</sup>DEI – Politecnico di Bari, via E. Orabona 4, 70125, Bari, Italy

## 6 **Abstract**

7 Microgrids are more and more called to satisfy, through the management of distributed  
8 generation sources and the electricity network, the demand for energy by local users.  
9 The simultaneous production of electrical and thermal energy by means of Combined  
10 Heat and Power (CHP) systems represents one of the features of a Microgrid and can  
11 contribute to improve system reliability, efficiency and economic performance. In this  
12 paper, an optimization procedure for day-ahead scheduling of a CHP-based Microgrid is  
13 developed, aiming to minimize operation and emission costs of Microgrid components  
14 in the presence of electric and thermal loads and renewable forecasts. To this purpose,  
15 four different operating strategies for CHP are accounted in Microgrid framework. The  
16 proposed methodology is based on a non-linear optimization technique and it is applied  
17 to the determination of day ahead operation program, with 15-minutes time step, for  
18 realistic model of an experimental Microgrid.

## 20 **Keywords**

21 Microgrid

---

\* Corresponding author.

Mail to: DEI – Politecnico di Bari, via E. Orabona 4, 70125, Bari, Italy

E-mail: [micheleantonio.trovato@poliba.it](mailto:micheleantonio.trovato@poliba.it)

Ph.: +39 080 5963244

Fax: +39 080 5963410

22 Combined Heat and Power

23 day-ahead scheduling

24 energy storage

25 distributed generation

26

27 **Nomenclature**

28 *Indices:*

29  $i$  Micro-Turbine based cogeneration system (MT)

30  $k$  Reciprocating-Engine based cogeneration system (RE)

31  $j$  Boiler

32  $s$  Energy Storage System (ESS)

33  $z$  Electrical Load

34  $h$  Thermal Load

35  $g$  Photovoltaic generator (PV)

36  $r$  Wind Turbine (WT)

37  $t$  Time period

38 *Parameters:*

39  $n_M$  Total number of MTs

40  $n_R$  Total number of REs

41  $n_B$  Total number of boilers

42  $n_S$  Total number of ESSs

43  $n_L$  Total number of electrical loads

44  $n_H$  Total number of thermal loads

- 45  $n_{PV}$  Total number of PVs
- 46  $n_{WT}$  Total number of WTs
- 47  $N$  Total number of time periods ( $t = 1, 2, \dots, N$ )
- 48 *Input Variables:*
- 49  $P_{zt}^L$  Electric power demand of  $z$ -th load in the  $t$ -th time period
- 50  $P_{gt}^V$  Electric power generated by  $g$ -th PV in the  $t$ -th time period
- 51  $P_{rt}^W$  Electric power generated by  $r$ -th WT in the  $t$ -th time period
- 52  $Q_{ht}$  Demand of  $h$ -th thermal load in the  $t$ -th time period
- 53 *State Variables:*
- 54  $P_{it}^M$  Electric power generated by  $i$ -th MT in the  $t$ -th time period
- 55  $P_{kt}^R$  Electric power generated by  $k$ -th RE in the  $t$ -th time period
- 56  $P_{st}^C$  Charging power of  $s$ -th ESS in the  $t$ -th time period
- 57  $P_{st}^D$  Discharging power of  $s$ -th ESS in the  $t$ -th time period
- 58  $E_{st}$  State Of Charge (SOC) of  $s$ -th ESS in the  $t$ -th time period
- 59  $P_{Pt}$  Electric power withdrawn from distribution network at Point of Common Coupling  
60 (PCC) in the  $t$ -th time period
- 61  $P_{Dt}$  Electric power delivered to distribution network at PCC in the  $t$ -th time period
- 62  $Q_{jt}^B$  Thermal power generated by the  $j$ -th boiler in the  $t$ -th time period
- 63 *Cost items:*
- 64  $C(P_{it}^M)$  operation cost of  $i$ -th MT in the  $t$ -th time period

- 65  $S(P_{it}^M)$  emission cost of  $i$ -th MT in the  $t$ -th time period
- 66  $C(P_{kt}^R)$  operation cost of  $k$ -th RE in the  $t$ -th time period
- 67  $S(P_{kt}^R)$  operation cost of  $k$ -th RE in the  $t$ -th time period
- 68  $C(Q_{jt}^B)$  operation cost of  $j$ -th boiler in the  $t$ -th time period
- 69  $S(Q_{jt}^B)$  emission cost of  $j$ -th boiler in the  $t$ -th time period
- 70  $C(P_{Pt})$  cost for electricity purchase at PCC
- 71  $R(P_{Dt})$  revenue for electricity delivery at PCC
- 72 *Constants:*
- 73  $\bar{P}_i^M, \underline{P}_i^M$  Maximum and minimum value of  $P_{it}^M$
- 74  $\bar{P}_k^R, \underline{P}_k^R$  Maximum and minimum value of  $P_{kt}^R$
- 75  $\bar{Q}_j^B, \underline{Q}_j^B$  Maximum and minimum value of  $Q_{jt}^B$
- 76  $\bar{P}_{Pt}, \bar{P}_{Dt}$  Maximum values of  $P_{Pt}$  and  $P_{Dt}$  at time  $t$
- 77  $\bar{P}_s^C, \bar{P}_s^D$  Maximum values of  $P_{st}^C$  and  $P_{st}^D$
- 78  $\bar{E}_s, \underline{E}_s$  Maximum and minimum value of  $E_{st}$
- 79  $\Delta t$  Amplitude of the  $t$ -th time period

80

## 81 **1. Introduction**

82 Microgrid (MG) is an ensemble of Distributed Generation (DG) technologies, Energy  
83 Storage Systems (ESSs) and electrical and thermal loads which can operate  
84 autonomously or in grid-connected mode. DG technologies typically include

85 photovoltaic (PV) and wind turbines (WT), microturbines (MT) and reciprocating  
86 internal combustion engines (RE).

87 The MG concept is based on two typical aspects: it is designed to supply electrical and  
88 thermal loads for a small community, operating as a controlled entity connected to the  
89 distribution network by the Point of Common Coupling (PCC) [1][2].

90 In general, the MG is monitored and controlled in real time through a hierarchical  
91 control structure including a central controller and local-source controllers. The central  
92 controller performs several functions at the highest level, such as energy management,  
93 security assessment, state estimation, protection coordination. Local controllers act in a  
94 coordinated way, to ensure each component to operate in its rated range and to carry out  
95 control strategies developed at central level [2].

96 In the field of energy management procedures, the optimal scheduling of MG operation  
97 is an attractive issue as regards the goal to be pursued (minimum-cost, maximum-profit  
98 and/or reliable operation) as well as the current MG configuration (grid-connected or  
99 islanded). Day-ahead scheduling is called to determine generation profiles of  
100 controllable sources according to forecast demand, whereas real time dispatching  
101 involves adjustments in order to smooth out load variation and renewable power  
102 fluctuations [3][4].

103 Different solutions have been proposed to approach the MG energy management  
104 problem. A thorough review of relevant methodologies, classified according to  
105 objective functions, optimization techniques, solution approaches and exploited  
106 software tools is reported in [5].

107 In [6], several operation strategies are shown, with the purpose of minimizing operation  
108 cost using DG sources only for periods in which using batteries is not convenient. In

109 [7], two strategies for the optimal management of ESS in a MG are proposed. An  
110 economic benefit maximization problem is considered in [8], where minimum on-off  
111 time constraints and ramping constraints are taken into account. In [9], user costs for  
112 Load Shedding are considered using PowerWorld Simulator®. A strategy for managing  
113 a MG containing PVs and hybrid ESSs is proposed in [10]. Whereas, an operation  
114 planning of MG considering time-of-use pricing is developed in [11], allowing to  
115 program the MG operation on the basis of electricity price trend. In [12], a multi-  
116 objective function is considered for environmental and economic optimization problem,  
117 in which pollutant emissions are taken into account through an equivalent cost. In [13],  
118 a multi-objective optimization integrated with network reconfiguration problem is  
119 executed. In [14], both day-ahead operational scheduling and unit commitment  
120 problems are considered in the presence of controllable loads. In [15], several objectives  
121 for microgrid optimal operation programming are weighed in a single function in order  
122 to prove the effectiveness of weighing coefficients.

123 Another crucial aspect in MG operation programming is the prediction of generated  
124 power from renewable sources. To this purpose, several methods based on Neural  
125 Networks are proposed in [16]. A stochastic approach is used in [17], to take into  
126 account prediction uncertainty in MG operation programming. Robust optimization is  
127 accounted in [18] to account for reserve needs to deal with possible deviations of wind  
128 generation from forecast levels, whereas load uncertainty and reliability costs are added  
129 in robust optimization in [19].

130 Recently, optimization of MG operation considering both electric and thermal demands  
131 has become of primary importance. In particular, the use of Combined Heat and Power  
132 (CHP) systems enforces the interactions among different energy forms and improve the

133 efficiency of energy supply in a MG [20]. For instance, in [21] CHP modelling is  
134 accounted along with an operating strategy of thermal storage in order to determine  
135 hourly MG plan. An advanced model of CHP, including cooling demand and involving  
136 ambient influence, is developed in [4]. The influence of heat pumps in the satisfaction  
137 of electric and thermal demand of a domestic MG is tackled in [22]. In [23] the optimal  
138 dispatch of microgrid with CHP is based on probabilistic algorithm accounting for load  
139 and renewable probability distribution function and with linear CHP costs, whereas in  
140 [24] the daily scheduling of CHP-based MG is based on a stochastic model involving  
141 CHP cost as quadratic function of electric and heat power production and considering  
142 feasible operating region linking electric and heat output typical of combined-cycle  
143 plants. Moreover, in [25] economic emission load dispatch scheduling in a MG with  
144 CHPs is based on quadratic cost function and the determination of emission merit order  
145 according to Differential Evolution Technique. In [26] linear formulation of the  
146 production cost function is provided in combination with the coordination cost to cover  
147 both heat and power demands. A linear problem of optimal scheduling of a CHP system  
148 in thermal following mode with energy storage is depicted in [27]. The influence of  
149 different charge schemes of electricity purchase on operation planning of energy smart  
150 homes including CHP is depicted in [28].

151 The aim of this work is to propose a procedure for optimal day-ahead operation  
152 scheduling of a MG, which is one of the tasks performed by MG Central Controller. A  
153 particular focus is devoted to proper modelling of CHP operation suitable for microgrid  
154 size and their integration with back-up boilers, in order to cover electric and thermal  
155 demand. A detailed characterization of MG components and electric/thermal load is  
156 provided, along with relevant suitable constraints, and differentiated costs for power



157 exchange from/to the distribution network at PCC are considered. The presence of  
158 several thermal loads in the same MG not connected to each other but sharing the  
159 electric production is considered as well. In addition, different operation strategies for  
160 CHP-based generators are embedded in the procedure, in order to prove the  
161 effectiveness of electric and thermal demand coverage assumptions. A non-linear  
162 formulation of day-ahead scheduling problem is provided and the procedure is  
163 implemented in MatLab adopting SQP solver. The proposed methodology is tailored to  
164 be implemented in a SCADA/EMS system of an experimental MG, and the paper  
165 presents the results of program development, planning to be implemented in a real MG  
166 facility. As compared to the approaches in literature dealing with the operation planning  
167 of CHP-based MG, the novel contributions of the paper are:

- 168 i) the characterization of typical operating modalities of CHP systems, as described  
169 in [29] and [30] for autonomous systems, in MG operation planning framework.  
170 These strategies are usually neglected in other formulations or only one of them is  
171 assumed [27][31];
- 172 ii) the adoption of realistic nonlinear efficiency functions for CHPs, instead of  
173 constant values as in [20][28][32][33];
- 174 iii) the integration in a single MG, sharing all electric production facilities, of several  
175 sources for the coverage of distinct thermal loads instead of considering a single  
176 aggregate thermal demand. Moreover, the presence of excess heat ensures higher  
177 flexibility [25][34];
- 178 iv) the analysis on day-ahead horizon with 15-min programming time step, more and  
179 more necessary to capture variations of renewable production [35], assuming the

180 presence of a second control stage, closer to real time operation, to deal with  
181 deviations from forecast values [36];

182 v) the exploitation of SQP method for the solution of the complete nonlinear  
183 optimization problem instead of mixed-integer linear programming that can lose  
184 information [37] or mixed-integer nonlinear programming that could not reach  
185 feasible point [38];

186 vi) the test of real CHP system operation integrated in an experimental MG.

187 The paper is organized as follows. In Section II, mathematical representation of MG  
188 components is proposed. Section III deals with MG day-ahead scheduling problem, and  
189 in Section IV test case and results are presented.

190

## 191 **2. Modeling of Microgrid components**

192 Exploitable technologies in a MG can be divided into different groups. Technologies  
193 based on non-programmable renewable energy sources (RES), such as wind speed, solar  
194 radiation and water flow, produce energy without significant control, therefore their  
195 contribution should be at most forecasted but could be affected by remarkable  
196 variations. An ESS can influence the operation of the MG by performing several tasks,  
197 such as improve the reliability and mitigate the uncertainty of electricity production by  
198 RESs. MTs and REs generate electrical power and useable exhaust heat which can  
199 provide hot water or process heat, and can run on a variety of fuels, allowing flexibility  
200 in the case of fuel unavailability and volatile fuel prices. Moreover, boilers usually  
201 compensate the action of CHP systems to cover thermal demand variations.

202 In this Section, models of MG components for the representation of economic and  
203 operation features in a day-ahead time interval are described. To this purpose, energy

204 production facilities based on non-programmable renewable energy sources have  
 205 generally negligible operation costs, since no buying cost is associated to the source,  
 206 whereas their production level in each interval of the day-ahead horizon is linked to  
 207 expected value of the forecast of source availability. Moreover, since they take part to  
 208 the MG that is a single entity interfacing the distribution network and eventually the  
 209 market, nor economic penalizations are ascribable to forecast errors neither specific  
 210 incentive schemes are accounted. On the other hand, programmable energy production  
 211 devices (e.g. fuel-based generation apparatus, as well as external network) can be fully  
 212 controlled but incur in remarkable short-term operation costs. Energy storage devices,  
 213 similarly to RES-based systems, have generally no variable cost, but are subject to  
 214 internal state variation and conversion losses.

215 The proposed distinction is reflected in the following formulation of device models for  
 216 day-ahead operation planning. In fact, WT and PV power production is linked to  
 217 ambient condition forecasts and no variable cost is accounted, whereas variable costs  
 218 are considered for MT, RE, boilers and grid connection. Storage devices involve loss  
 219 terms with no variable cost.

## 220 **2.1. Wind turbine**

221 The power output of the  $r$ -th WT in the  $t$ -th time interval, according to a given value of  
 222 wind speed  $v_{rt}$ , depending on ground clearance and roughness, is evaluated as follows:

$$223 \quad P_{rt}^W = \begin{cases} f(v_{rt}) & \underline{v}_r \leq v_{rt} \leq \tilde{v}_r \\ \tilde{P}_r^W & \tilde{v}_r \leq v_{rt} \leq \bar{v}_r \\ 0 & \text{else} \end{cases} \quad (1)$$

224 where  $\tilde{P}_r^W$  is the rated power of the WT,  $\underline{v}_r, \tilde{v}_r, \bar{v}_r$  are the cut-in, rated and cut-off wind  
 225 speed, respectively, and  $f(v_{rt})$  is a polynomial function representing power-speed  
 226 curve of the WT. Suitable forecasting procedure or historical data can be exploited to  
 227 obtain  $v_{rt}$  over a time interval [39].

## 228 **2.2. Photovoltaic generator**

229 The output power of the  $g$ -th PV generator at the  $t$ -th time interval is expressed as  
 230 follows:

$$231 \quad P_{gt}^V = \gamma_g \cdot n_g^V \cdot \zeta_g^V(\theta_{gt}) \cdot A_g \cdot I_{gt} \quad (2)$$

232 where  $I_{gt}$  [kW/m<sup>2</sup>] is the incident irradiance on panel surface, taking into account  
 233 direct, diffuse and reflected components [40],  $A_g$  [m<sup>2</sup>] is the panel area,  $n_g^V$  is the  
 234 number of panels in the PV system,  $\zeta_g^V(\theta_{gt})$  is panel efficiency depending on its  
 235 temperature  $\theta_{gt}$  [41], and  $\gamma_g$  is a degradation coefficient accounting for shading,  
 236 inverter and asymmetries losses. Solar irradiance can be estimated according to forecast  
 237 procedures or historical data [42].

## 238 **2.3. Energy storage system**

239 The operation of an ESS is characterized by its energy content, or State Of Charge  
 240 (SOC). The SOC of the  $s$ -th ESS in  $t$ -th time stage is related to capacity left at previous  
 241 stage  $t_-$ , as follows:

$$242 \quad E_{st} = (1 - q_s^D) \cdot E_{st_-} + \left( P_{st}^C \cdot \Delta t \cdot \psi_s^C(P_{st}^C) \right) - \left( \frac{P_{st}^D \cdot \Delta t}{\psi_s^D(P_{st}^D)} \right) \quad (3.a)$$

243 where  $\psi_s^C(P_{st}^C)$  and  $\psi_s^D(P_{st}^D)$  are the charging and the discharging efficiency of the  $s$ -

244 th ESS, respectively, depending on charge and discharge power level, and the self-  
 245 discharging effect is accounted by means of a quota  $q_s^D$  of available capacity at previous  
 246 stage [43][44]. At the first time step,  $t=1$ , it is assumed that  $t_- = N$  so that the same  
 247 state is present at the extremes of the day. Moreover, the following relation holds, in  
 248 order to fix the SOC at the beginning of programming horizon to a value  $E_s'$  able to  
 249 guarantee an efficient daily operation in any condition.

$$250 \quad E_{sN} = E_s' \quad (3.b)$$

251 The values of SOC and charge/discharge power are limited by technical features and  
 252 defined operating conditions of the ESS, as follows:

$$253 \quad \underline{E}_s \leq E_{st} \leq \bar{E}_s \quad (4.a)$$

$$254 \quad 0 \leq P_{st}^C \leq \bar{P}_s^C \quad (4.b)$$

$$255 \quad 0 \leq P_{st}^D \leq \bar{P}_s^D \quad (4.c)$$

256 In particular, maximum SOC value in equation (4.a) is determined as  $\bar{E}_s = \mu_s \cdot E_s^{nom}$   
 257 where  $E_s^{nom}$  is the nameplate energy capacity of the ESS and  $\mu_s$  represents the capacity  
 258 reduction factor. This factor depends on the utilization history of the ESS, i.e.  
 259 equivalent cycles at the defined depth of discharge [45][46][47], from the beginning of  
 260 exploitation, and it is updated for the analysis of different days.

261 Moreover, for each time interval, it is assumed that the ESS could only be charged or  
 262 discharged. Therefore, the following condition holds:

$$263 \quad P_{st}^C \cdot P_{st}^D = 0 \quad (4.d)$$

## 264 **2.4. MicroTurbine based Cogeneration System**

265 The operation cost of  $i$ -th MT can be evaluated as follows [48]:

$$266 \quad C(P_{it}^M) = \varphi_i^M \cdot \frac{\Delta t \cdot P_{it}^M}{H_i^M \cdot \eta_i(P_{it}^M)} \quad (5)$$

267 where  $\varphi_i^M$  [€ per fuel unit] is the cost of fuel (generally natural gas),  $H_i^M$  [kWh per  
268 fuel unit] is the lower heating value of fuel and  $\eta_i(P_{it}^M)$  is the electrical efficiency at  
269 specific level of power production  $P_{it}^M$ . The latter has to be within technical limits of  
270 the MT:

$$271 \quad \underline{P}_i^M \leq P_{it}^M \leq \bar{P}_i^M \quad (6)$$

272 Whenever the  $i$ -th MT operates in CHP mode, its exploitable thermal output in the  $t$ -th  
273 time stage  $Q_{it}^M$  can be obtained by the following expression [49]:

$$274 \quad Q_{it}^M = P_{it}^M \cdot \frac{\xi_i^M}{\eta_i(P_{it}^M)} \quad (7)$$

275 where  $\xi_i^M$  represents the thermal efficiency.

276 In order to determine a proper tradeoff between fuel expenses and pollutant emissions,  
277 the equivalent cost of CO<sub>2</sub> emissions is employed, by means of a unit penalty cost  $\sigma_E$   
278 [€/kg]. The equivalent emission cost of the  $i$ -th MT can be evaluated as follows:

$$279 \quad S(P_{it}^M) = \sigma_E \cdot \varepsilon_i(P_{it}^M) \cdot \Delta t \cdot P_{it}^M \quad (8)$$

280 where  $\varepsilon_i(P_{it}^M)$  [kg/kWh] is the emission factor of the  $i$ -th MT, determined as  
281  $\varepsilon_i(P_{it}^M) = \bar{\varepsilon}_i^M / \eta_i(P_{it}^M)$ , being  $\bar{\varepsilon}_i^M$  a constant emission factor depending on the burnt  
282 fuel in the  $i$ -th MT.

283 Moreover, ramping limits can be neglected in the day-ahead horizon with reasonably  
284 wide time step [4].

### 285 **2.5. Reciprocating-Engine based Cogeneration System**

286 The operation cost of  $k$ -th RE system in the  $t$ -th time stage can have the following  
287 expression [50]:

$$288 \quad C(P_{kt}^R) = \varphi_k^R \cdot \frac{\Delta t \cdot P_{kt}^R}{H_k^R \cdot \eta_k(P_{kt}^R)} \quad (9)$$

289 where  $\varphi_k^R$  [€ per fuel unit] is the fuel cost,  $H_k^R$  [kWh per fuel unit] is the lower heating  
290 value of fuel,  $\eta_k(P_{kt}^R)$  is the electrical efficiency. Power production of the RE  $P_{kt}^R$  is  
291 limited by technical features:

$$292 \quad \underline{P}_k^R \leq P_{kt}^R \leq \bar{P}_k^R \quad (10)$$

293 Moreover, in CHP mode, the useable thermal power from  $k$ -th RE system at the  $t$ -th  
294 time interval  $Q_{kt}^R$  can be evaluated as follows [49]:

$$295 \quad Q_{kt}^R = P_{kt}^R \cdot \frac{\xi_k^R}{\eta_k(P_{kt}^R)} \quad (11)$$

296 where  $\xi_k^R$  is the thermal efficiency.

297 The equivalent cost of CO<sub>2</sub> emissions can be calculated as:

$$298 \quad S(P_{kt}^R) = \sigma_E \cdot \varepsilon_k(P_{kt}^R) \cdot \Delta t \cdot P_{kt}^R \quad (12)$$

299 where  $\varepsilon_k(P_{kt}^R)$  [kg/kWh] is the emission factor of the  $k$ -th RE, determined as

300  $\varepsilon_k(P_{kt}^R) = \bar{\varepsilon}_k^R / \eta_k(P_{kt}^R)$ , being  $\bar{\varepsilon}_k^R$  a constant emission factor depending on the burnt fuel  
301 in the  $k$ -th RE.

302

## 303 2.6. Boiler

304 The operation cost of the  $j$ -th boiler in the  $t$ -th time stage can be expressed as [51]:

$$305 \quad C(Q_{jt}^B) = \varphi_j^B \cdot \frac{\Delta t \cdot Q_{jt}^B}{H_j^B \cdot \xi_j^B} \quad (13)$$

306 where  $\varphi_j^B$  is the fuel cost [€ per fuel unit],  $H_j^B$  [kWh per fuel unit] is the lower heating  
 307 value,  $\xi_j^B$  is the thermal efficiency. The thermal power produced by the  $j$ -th boiler  $Q_{jt}^B$   
 308 is limited in the range:

$$309 \quad \underline{Q}_j^B \leq Q_{jt}^B \leq \bar{Q}_j^B \quad (14)$$

310 The equivalent cost of CO<sub>2</sub> emissions from the  $j$ -th boiler can be evaluated by the  
 311 expression:

$$312 \quad S(Q_{jt}^B) = \sigma_E \cdot \varepsilon_j(Q_{jt}^B) \cdot \Delta t \cdot Q_{jt}^B \quad (15)$$

313 where  $\varepsilon_j(Q_{jt}^B)$  [kg/kWh] is the emission factor of the  $j$ -th boiler referred to thermal  
 314 power production.

## 315 2.7. Power exchange at PCC

316 In the grid-connected mode, the cost of electric energy withdrawal at PCC from the  
 317 distribution network in the  $t$ -th time step is given by the expression:

$$318 \quad C(P_{Pt}) = \pi_{Pt} \cdot \Delta t \cdot P_{Pt} \quad (16)$$

319 where  $\pi_{Pt}$  [€/kWh] is the electricity purchase price, and  $P_{Pt}$  is limited by a constraint  
 320 deriving from contractual conditions of energy purchase:

$$321 \quad 0 \geq P_{Pt} \geq \bar{P}_{Pt} \quad (17)$$

322 Whereas, the revenue from the energy delivered at PCC to the distribution network can



323 be put in the form:

$$324 \quad R(P_{Dt}) = k_D \cdot \pi_{Dt} \cdot \Delta t \cdot P_{Dt} \quad (18)$$

325 where  $\pi_{Dt}$  is the electricity selling price,  $k_D < 1$  is a coefficient that takes into account  
326 the economic burden of connection service [52]. Analogously to power purchase, the  
327 delivered amount  $P_{Dt}$  has to be below a contractual fixed value:

$$328 \quad 0 \geq P_{Dt} \geq \bar{P}_{Dt} \quad (19)$$

329 In order to avoid bidirectional power exchange at PCC in a single  $t$ -th time interval, the  
330 following condition holds:

$$331 \quad P_{Pt} \cdot P_{Dt} = 0 \quad (20)$$

332

### 333 **3. Day-ahead energy management problem**

334 In this Section, a nonlinear optimization procedure is formulated for the day-ahead  
335 scheduling of the MG generation sources in order to meet the internal electric and  
336 thermal demand by minimizing operation costs and environmental impacts.

#### 337 **3.1. Problem formulation**

338 The MG energy management function is performed through the solution of a non-linear  
339 optimization problem, aiming to minimize an objective function subject to equality and  
340 inequality constraints, that can be posed in the following canonical form:

$$341 \quad \begin{aligned} & \min_{\mathbf{x}} J(\mathbf{x}) \\ & \text{subject to } \begin{cases} \mathbf{g}(\mathbf{x}) = \mathbf{0} \\ \mathbf{h}(\mathbf{x}) \leq \mathbf{0} \end{cases} \end{aligned} \quad (21)$$

342 where  $\mathbf{x}$  is a  $(n_M + n_R + n_B + 3 \cdot n_S + 2) \cdot N$  dimensional vector including the subsets of

343 variables  $\{P_{it}^M\}, \{P_{kt}^R\}, \{Q_{jt}^B\}, \{P_{st}^C\}, \{P_{st}^D\}, \{E_{st}\}, \{P_{Pt}\}, \{P_{Dt}\}$  and  $J(\mathbf{x})$  includes the  
 344 MG operation and emission costs over the total time interval  $N \cdot \Delta t$ , expressed as  
 345 follows:

$$346 \quad J(\mathbf{x}) = \sum_{t=1}^N \left\{ C(P_{Pt}) - R(P_{Dt}) + \sum_{i=1}^{n_M} [C(P_{it}^M) + S(P_{it}^M)] + \right. \quad (22)$$

$$\left. + \sum_{k=1}^{n_R} [C(P_{kt}^R) + S(P_{kt}^R)] + \sum_{j=1}^{n_B} [C(Q_{jt}^B) + S(Q_{jt}^B)] \right\}$$

347 Equality constraints in (21) include the subsets: (3.a), giving out  $n_S \cdot N$  linear relations  
 348 for all storage devices in the whole time horizon; (3.b), with  $n_S$  linear equations; (4.d),  
 349 constituting  $n_S \cdot N$  non-linear conditions; (20), corresponding to  $N$  non-linear  
 350 constraints. Moreover, the electrical power balance of the MG in the  $t$ -th time period is  
 351 imposed, requiring that the sum of load demand of all electricity users taking part to the  
 352 MG and net power interchange with the distribution network equals the production of  
 353 internal energy sources, neglecting MG losses in the day-ahead programming stage, as  
 354 follows:

$$355 \quad \sum_{z=1}^{n_L} P_{zt}^L + (P_{Dt} - P_{Pt}) = \sum_{i=1}^{n_M} P_{it}^M + \sum_{k=1}^{n_R} P_{kt}^R + \sum_{s=1}^{n_S} (P_{st}^D - P_{st}^C) + \sum_{g=1}^{n_{PV}} P_{gt}^V + \sum_{r=1}^{n_{WT}} P_{rt}^W \quad (23)$$

356 By considering that the electricity balance over all the planning horizon involves  $N$   
 357 linear constraints, the set of equality constraints  $\mathbf{g}(\mathbf{x}) = \mathbf{0}$  includes  $(2 \cdot n_S + 2) \cdot N + n_S$   
 358 relations.

359 Furthermore, inequality constraints in (21) are represented by the subsets: (4.a)-(4.c),  
 360 constituting  $6 \cdot n_S \cdot N$  linear conditions; (6), involving  $2 \cdot n_M \cdot N$  linear relations; (10),

361 yielding  $2 \cdot n_R \cdot N$  linear constraints; (14), constituting  $2 \cdot n_B \cdot N$  linear inequalities; (17)  
 362 and (19), giving rise to  $2 \cdot N$  linear relations each. Moreover, thermal power balance is  
 363 dealt with, accounting for the technologies involved in thermal energy production, i.e.  
 364 CHP units and Boilers. In accordance with the operation criteria of the MG, the  
 365 possibility that a part of thermal energy can be released to the atmosphere at a given  
 366 time period is considered. In particular, it is supposed that a part of the exhaust air after  
 367 combustion, controlled by means of valves, passes through the exchangers to give  
 368 useful heat, and a ventilation system, whose electric demand can be considered  
 369 negligible, lets exhausts leave the thermal supply. In addition, the presence of different  
 370 thermal loads, i.e. groups of users served by a determined subset of thermal power  
 371 sources in the MG framework, is accounted. The link between the  $h$ -th thermal load and  
 372 the thermal power sources of MG at the  $t$ -th time period can be expressed by the  
 373 following inequality:

$$374 \quad Q_{ht} \leq \sum_{i=1}^{n_M} a_{hi}^M \cdot Q_{it}^M + \sum_{k=1}^{n_R} a_{hk}^R \cdot Q_{kt}^R + \sum_{j=1}^{n_B} a_{hj}^B \cdot Q_{jt}^B \quad (24)$$

375 where  $Q_{it}^M$  and  $Q_{kt}^R$  are evaluated by the non-linear expressions (7) and (11),  
 376 respectively. Moreover, the coefficients  $a_{hi}^M$ ,  $a_{hk}^R$  and  $a_{hj}^B$  are equal to 1 if the  
 377 correspondent  $i$ -th MT,  $k$ -th RE or  $j$ -th boiler, respectively, is connected to the  $h$ -th  
 378 thermal load, otherwise they are equal to zero.

379 Since the thermal power balance for all thermal users over the planning horizon  
 380 involves  $n_H \cdot N$  non-linear relations, the size of inequality constraint set  $\mathbf{h}(\mathbf{x}) \leq \mathbf{0}$  is

$$381 \quad (2 \cdot n_M + 2 \cdot n_R + 2 \cdot n_B + 6 \cdot n_S + n_H + 4) \cdot N.$$

382 The described methodology has the advantage to include a wide set of the technologies  
383 taking part to a MG, and slight variations can allow to model other specific devices. The  
384 adopted models allow to catch the behaviour of MG-sized devices in the day-ahead  
385 horizon, where the ramping limits can be neglected and steady-state conditions can be  
386 considered valid for each time step. Moreover, it is worth to remark that the procedure  
387 is able to simulate the islanded mode condition of MG operation in defined time steps,  
388 by assuming  $\bar{P}_{Pt} = 0$  and  $\bar{P}_{Dt} = 0$ . This implies that grid costs do not affect the objective  
389 function in that specific time period and the electricity balance cannot rely on flexibility  
390 ensured by distribution network exchange. Hence, the optimal day-ahead operation plan  
391 is determined on the basis of the sole MG internal sources.

### 392 **3.2. CHP Operation Strategies**

393 The solution of problem (21) provides the optimal values of the outputs of CHP devices,  
394 boilers and ESS, on the basis of expected contributions by PV and WT systems, to  
395 satisfy the load demand.

396 However, ad hoc strategies for managing CHP units can be required to improve long-  
397 term technology performance and to comply with specific needs [30]:

398 C1. *electrical load tracking*: selected CHP units are managed with the aim of  
399 following the evolution of electricity load;

400 C2. *thermal load tracking*: specified CHP units are operated with the objective of  
401 following the behavior of defined heating loads;

402 C3. *on-off operation*: given CHP units are operated at the rated output over defined  
403 time periods.

404 The C1 strategy can be easily handled, by adding to the problem (21), for each time

405 stage, the following equality constraint:

$$406 \quad \alpha_t \cdot \sum_{z=1}^{n_L} P_{zt}^L = \left[ \sum_{i=1}^{n_M} b_{it}^M \cdot P_{it}^M + \sum_{k=1}^{n_R} b_{kt}^R \cdot P_{kt}^R \right] \cdot \beta_t \quad (25)$$

407 where the coefficient  $\alpha_t$  ( $0 \leq \alpha_t \leq 1$ ) represents the portion of electrical load that is  
 408 covered at the  $t$ -th stage by the  $i$ -th MT or the  $k$ -th RE, selected by imposing the binary  
 409 factors  $b_{it}^M$  and  $b_{kt}^R$ , respectively, equal to 1. At the  $t$ -th time step, the C1 strategy is  
 410 activated by  $\beta_t = 1$  and  $\alpha_t \neq 0$ , whereas, as long as  $\beta_t = 0$ ,  $\alpha_t = 0$  and C1 strategy is  
 411 not applied. Therefore, the activation of C1 strategy yields the increase of equality  
 412 constraints to a total of  $(2 \cdot n_S + 3) \cdot N + n_S$  relations.

413 The C2 strategy is modeled by introducing, for the  $h$ -th thermal load and for the  $t$ -th  
 414 time step, the following equality condition:

$$415 \quad \alpha_{ht} \cdot Q_{ht} = \left[ \sum_{i=1}^{n_M} u_{it}^M \cdot a_{hi}^M \cdot Q_{it}^M + \sum_{k=1}^{n_R} u_{kt}^R \cdot a_{hk}^R \cdot Q_{kt}^R \right] \cdot \beta_{ht} \quad (26)$$

416 where the coefficient  $\alpha_{ht}$  ( $0 \leq \alpha_{ht} \leq 1$ ) represents the portion of  $h$ -th thermal load that is  
 417 fed at the  $t$ -th step by the  $i$ -th MT or the  $k$ -th RE selected by imposing the binary factors  
 418  $u_{it}^M$  and  $u_{kt}^R$ , respectively, equal to 1. At the  $t$ -th time step and for the  $h$ -th thermal load,  
 419 the C2 strategy is in force if  $\beta_{ht} = 1$  and  $\alpha_{ht} \neq 0$ , whereas, as long as  $\beta_{ht} = 0$ ,  $\alpha_{ht} = 0$   
 420 and C2 strategy is not applied. Therefore, the presence of C2 strategy involves a total of  
 421  $(2 \cdot n_S + 2 + n_H) \cdot N + n_S$  equality constraints.

422 The C3 strategy can be implemented by introducing, for the  $i$ -th MT and/or the  $k$ -th RE,  
 423 the following relations:

424 
$$\beta_{it}^M \cdot P_{it}^M = \beta_{it}^M \cdot \bar{P}_{it}^M \quad (27.a)$$

425 
$$\beta_{kt}^R \cdot P_{kt}^R = \beta_{kt}^R \cdot \bar{P}_{kt}^R \quad (27.b)$$

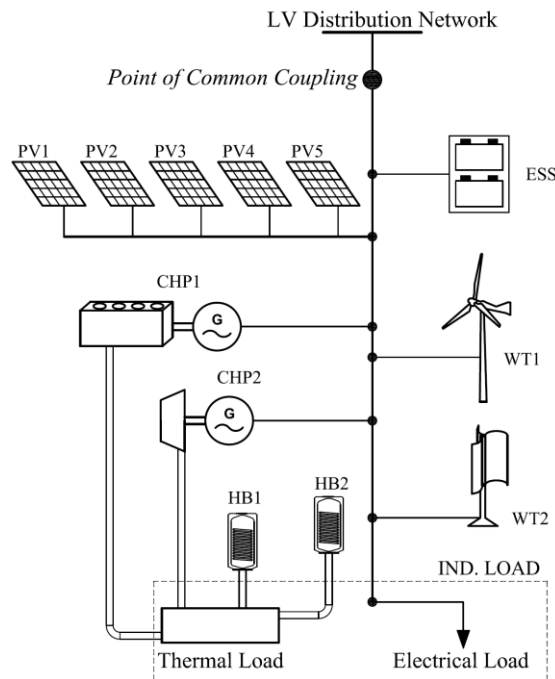
426 The strategy is activated, for the  $i$ -th MT or the  $k$ -th RE, if for the  $t$ -th time step, the  
 427 binary factors  $\beta_{it}^M$  or  $\beta_{kt}^R$  is equal to 1, respectively. Whereas, as long as  $\beta_{it}^M = 0$  or  
 428  $\beta_{kt}^R = 0$ , the C3 strategy is not applied. Therefore, the presence of C3 strategy involves a  
 429 total of  $(2 \cdot n_S + 2 + n_M + n_R) \cdot N + n_S$  equality constraints.

430

431 **4. Test Results**

432 **4.1. The test MG under study**

433 The proposed optimization procedure and CHP strategies are applied to the test MG  
 434 shown in Fig. 1.



435

436

Fig. 1. The test MG.

437

438 The test MG represents a selected configuration of experimental facility built at Power  
439 and Energy System laboratory of Politecnico di Bari thanks to EU funds [53] with  
440 improved thermal section, currently under integration. The experimental facility is a  
441 low-voltage network, that can be operated in grid-connected or islanded mode,  
442 including the following devices:

443 - a gas-fueled CHP system, equipped with two variable-speed REs with total 105  
444 kW rated electric power;

445 - a gas MT with 30 kW nominal power;

446 - a 50-kW photovoltaic field composed of five sub-arrays with different panel  
447 technologies;

448 - a sodium-nickel battery working at roughly 260 °C, with a discharge duration of  
449 3 hours;

450 - a 60-kVA wind turbine emulator, based on a back-to-back converter controlled  
451 according to models of different mini-wind generators and to measurement of an  
452 anemometer;

453 - two programmable loads, with 150 kVA rated power each, able to replicate  
454 active and reactive power needs of different kinds of load;

455 - a by-pass converter, with 200 kVA rated power, which allows the power  
456 exchange with the main network to be fixed at a specified value.

457 The facility is equipped with a Modbus/TCP-IP communication network, and it is  
458 monitored and controlled by means of a proper SCADA/EMS system, based on a

459 hierarchical structure [54]. The proposed day-ahead operation planning function is  
 460 aimed to be implemented in the SCADA system by means of software integration  
 461 ensured by Open Platform Communication (OPC) environment. Therefore, the  
 462 proposed procedure is currently object of real-world implementation.

463 The main characteristics of test MG components for the relations described in Section 2  
 464 are described in Table 1 for renewable-based components and in Table 2 for other  
 465 devices. For the employed ESS, available depth of discharge is 80%, self-discharging  
 466 effect is assumed negligible in the daily time horizon, charge and discharge efficiencies  
 467 are observed to be quite independent on power levels, and no previous exploitation is  
 468 assumed, therefore ESS maximum SOC is equal to rated capacity. The amount of power  
 469 exchange at PCC is capped at 200 kW on both withdrawal and delivery.

470

471

472

Table 1. Characteristics of renewable devices in the Test MG

Device Name	Description	Rated electric power [kW]	Cut-in / Nominal / Cut-off wind speed [m/s]	PV panel power [W] / module number / nominal efficiency [%]
<i>WT1</i>	33-kW horizontal axis wind turbine	33	3.5 / 11 / 20	
<i>WT2</i>	two 6-kW vertical axis wind turbines	12	5 / 14 / 25	
<i>PV1</i>	photovoltaic triple junction a-Si modules	9.216		144 / 64 / 7.7
<i>PV2</i>	photovoltaic mono-crystalline Si modules	10.53		270 / 39 / 16.6
<i>PV3</i>	photovoltaic poly-crystalline Si modules	10.5		250 / 42 / 15.4
<i>PV3</i>	photovoltaic CIS technology	9.6		150 / 64 / 12.2
<i>PV3</i>	photovoltaic mono N-type modules	9.9		300 / 33 / 18.3

473

474

Table 2. Characteristics of non-renewable devices in the Test MG

Device Name	Description	Rated electric (charge/discharge) power [kW]	Rated thermal power [kW]	Rated capacity [kWh]	Rated electric (charge/discharge) efficiency	Rated thermal efficiency
<i>ESS</i>	sodium-nickel chloride battery system	44 / 48	---	141	85% / 85%	---
<i>CHP1</i>	gas-fuelled RE in cogeneration mode	105	180	---	31.5% (Fig. 2)	50%
<i>CHP2</i>	gas MT in cogeneration mode	28	57	---	24.8% (Fig. 2)	50%
<i>B1</i>	wood-fuelled boiler		20			82.5%
<i>B2</i>	pellet-fuelled boiler		75			88.2%

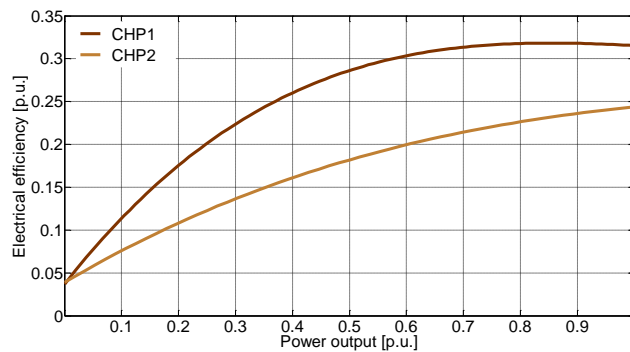
475



476 The electric efficiency trends of CHP systems according to power production level are  
 477 expressed by means of the following third-order polynomial equations and their trends  
 478 are depicted in Fig. 2 according to power output in p.u. of nominal power:

$$479 \text{ CHP1: } \eta_k(P_{kt}^R) = 2.21e-7 \cdot (P_{kt}^R)^3 - 7.47e-5 \cdot (P_{kt}^R)^2 + 8.06e-3 \cdot (P_{kt}^R) + 3.707e-2 \quad (28.a)$$

$$480 \text{ CHP2: } \eta_i(P_{it}^M) = 2.22e-6 \cdot (P_{it}^M)^3 - 3e-4 \cdot (P_{it}^M)^2 + 1.397e-2 \cdot (P_{it}^M) + 3.905e-2 \quad (28.b)$$



481

482

Fig. 2. Electric efficiency trends of CHP systems in the test MG.

483

484 Thermal efficiency has been considered constant to the rated values reported in Table 2

485 both for CHP and boilers, since no remarkable variations are observed during operation.

486 Emission factor for gas burning in CHP1 and CHP2 involves

487  $\bar{\varepsilon}_k^R = \bar{\varepsilon}_i^M = 0.1404 \text{ kg/kWh}_{\text{pr}}$  obtaining, at nominal power, 0.453 kg/kWh for CHP1 and

488 0.560 kg/kWh for CHP2, according to the nameplate data. Whereas, emission factor for

489 boilers is constant, though suitably low (0.002 kg/kWh) due to the exploitation of

490 renewable fuels, whose burning is not related to proper emissions.

491 Moreover, for each CHP, the minimum production level is set to zero, compatibly to the

492 observed low minimum stable production (roughly 1 kW). Daily curves of electrical and

493 thermal load demand are taken from data of industrial users by an Italian distribution

494 company. Weather data for the forecast of renewable sources production are taken from

495 meteorological stations placed in the considered location [55]. Electric energy  
496 purchasing price is determined as the sum of market prices and service costs according  
497 to Italian rules, whereas electric energy selling price is defined by the Italian energy  
498 authority [52]. Finally, fuel costs are constant and derive from data by a fuel distribution  
499 company [56] and are equal to 0.51 €/m<sup>3</sup> for gas, 0.17 €/kg for wood, 0.32 €/kg for  
500 pellet, and emission cost is equal to 5.7 €/t [57].

501 The proposed non-linear optimization methodology is implemented, dividing the day  
502 into  $N = 96$  time steps of 15 minutes each, in MatLab® environment and solved through  
503 *fmincon* function in Optimization Toolbox exploiting SQP method [58], that has been  
504 proved robust for the solution of nonlinear optimization problems, even in non-convex  
505 formulations, and it is characterized by superlinear convergence [59][60]. The SQP  
506 method is based on the formulation, for each major iteration, of a Quadratic  
507 Programming subproblem based on a quadratic approximation of the Lagrangian  
508 function with positive semidefinite Hessian matrix and linearized constraints, whose  
509 solution is used to form a search direction for a line search procedure with step length  
510 according to a merit function [61][62]. As a nonlinear programming method, SQP  
511 efficiently looks for a local solution, and the solution search is improved starting from a  
512 feasible initial point [62]. In the proposed procedure the initial point is obtained by  
513 solving a linearized version of the problem, as suggested in [63]. The linearized  
514 problem is built by assuming efficiencies at rated levels, irrespective of power amount,  
515 in (3.a), (5), (7), (8), (9), (11), (12), and neglecting nonlinear constraints (4.d) and (20)  
516 on bidirectional power flow.

517

#### 518 **4.2. Test Cases**

519 Simulations are carried out according to data of a typical summer working day, where  
520 forecast electricity load amounts to 3,422 kWh in the whole day with a power peak of  
521 165 kW at hour 18. A quota of 14.4% of daily load is covered by forecast RES  
522 production, with a peak of 60 kW at hour 12. Moreover, a single thermal load is  
523 accounted, analogously to the situation of the experimental facility. It amounts to 4,329  
524 kWh with a maximum of 215 kW at hour 18. ESS initial SOC is set to 0.80 p.u. of rated  
525 capacity. Trends of electricity price for the day under investigation are shown in Fig. 3.  
526 It is worth to remark that purchasing price varies on hourly basis according to market  
527 influence, whereas selling price assumes only 3 different values in the day.



Fig. 3. Electricity price.

528  
529  
530 Simulations are carried out by applying each CHP strategy described in Section 3.2, and  
531 relevant results are compared to the reference solution of the problem reported in  
532 Section 3.1 (Base Case).

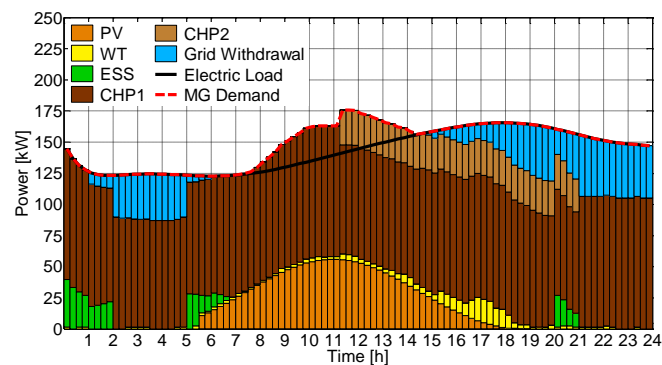
#### 4.2.1. Base Case

533  
534 The diagrams of electric power balance and thermal power balance for the Base Case  
535 are shown in Figs. 4 and 5, respectively. It can be pointed out that, for the considered  
536 day, 75.0% of the daily electric load is satisfied by CHP systems, 8.0% by electricity  
537 exchange at PCC, and the share of ESS is 2.8% and is concentrated in early morning  
538 and in peak price period in the evening. The sum of these contributions and RES-based

539 production (14.4%, as previously stated) exceeds the total daily load, since the  
540 supplemental share (3.8%) relates to the charging of the ESS in central hours of the day,  
541 and this is ascribable to the compliance with the constraint (3.b). This yields an increase  
542 of total MG electricity demand (sum of electric load and ESS charge power), shown in  
543 red dashed line in Fig. 4.

544 The coverage of thermal load is mainly performed by CHPs, with 83.6% contribution of  
545 RE (CHP1) and 12.9% by MT (CHP2). These systems work in a different manner, since  
546 CHP1 behaves according to load variations, whereas CHP2 is off in early morning and  
547 evening, and in central hours of the day it runs at maximum power output. Moreover,  
548 B1 helps covering morning peak, contributing by 3.2% to cover thermal load demand,  
549 whereas 0.3% of load is covered by B2 in central hours of the day, before CHP2 is on.

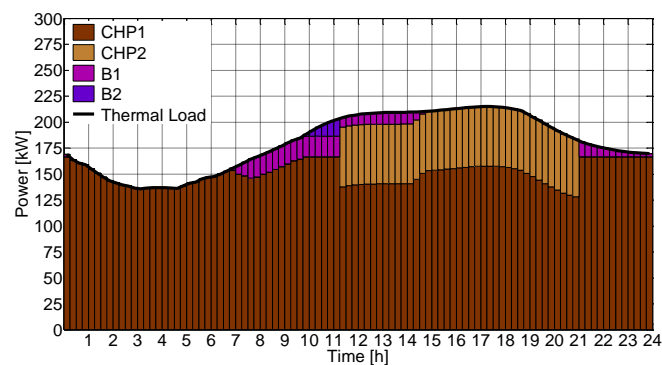
550



551

552

Fig. 4. Base Case Strategy: electrical power balance.



553

554 Fig. 5. Base Case Strategy: thermal power balance.

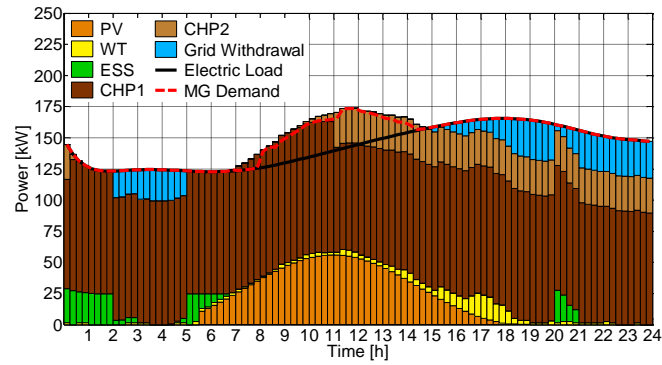
555

#### 556 **4.2.2. Electrical Load Tracking – C1 Strategy**

557 In order to prove the C1 strategy proposed in Section 3.2, eq. (25) is considered in  
558 equality constraints, assuming  $\alpha_t = 0.8$  and involving both CHP systems over the whole  
559 day ( $b_{it}^M = 1$  and  $b_{kt}^R = 1 \quad \forall t$ ). Complying with this requirement, the sum of CHP  
560 contributions covers the 80% of electric load profile for each time step of the considered  
561 day, as can be noted in Fig. 6. CHP1 and CHP2 cover 69.0% and 11.0% of load,  
562 respectively, and their contributions are shared according to load profile, since the  
563 modulation is mainly performed by CHP1 during off-peak load, whereas CHP2 is run  
564 almost close to nominal value in the second half of the day. Whereas 2.8% of daily  
565 electric load is satisfied by ESS and 7.4% by electricity exchange at PCC. The total MG  
566 demand is 3.8% higher than load, due to ESS charging. Moreover, 0.8% of internal  
567 production is sold to the grid in central hours of the day (i.e. when renewables exceed  
568 the remaining 20% of load), and this is reported in Fig. 6 as the difference between the  
569 envelope of bars and the dashed red curve.

570 Thermal power balance is illustrated in Fig. 7. In this case, thermal load is mainly  
571 satisfied by CHP systems, and an excess thermal power is registered (roughly 5.9% of  
572 the total daily amount), especially in the morning and in the presence of peak electric  
573 load, as a by-product of electric load tracking. B2 is off over the whole day and B1  
574 contributes only by 1.4% to load coverage in peak intervals, when the contemporaneous  
575 extra-production by RES does not allow CHPs to produce more thermal power.

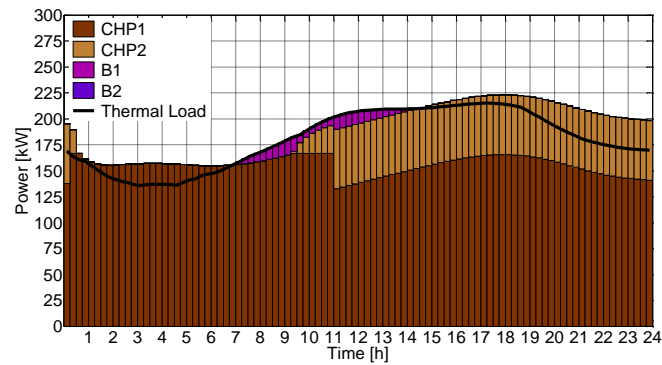
576



577

578

Fig. 6. C1 Strategy: electrical power balance.



579

580

Fig. 7. C1 Strategy: thermal power balance.

581

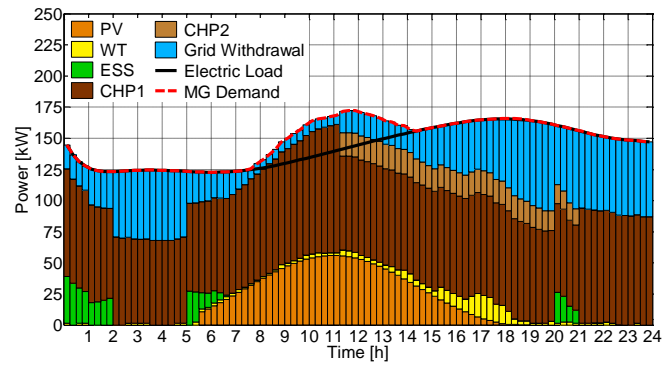
#### 582 4.2.3. Thermal Load Tracking – C2 Strategy

583 The C2 strategy described in Section 3.2 is implemented by adding eq. (26) to the set of  
 584 equality constraints and setting the coefficient  $\alpha_{ht} = 0.8$  for the whole day. Both CHP  
 585 systems are involved in the strategy, i.e.  $u_{it}^M = 1$  and  $u_{kt}^R = 1 \forall t$ .

586 The relevant electric power sharing is illustrated in Fig. 8. It can be noted that 61.6% of  
 587 electric load is matched by CHP systems, 25.0% by electricity exchange at PCC and the  
 588 contribution of ESS is less intense, at 2.7%. The total MG demand is 3.7% higher than  
 589 load profile, corresponding to ESS charge, and no grid injection is observed.

590 Thermal power balance is reported in Fig. 9. It can be observed that CHP units share the  
 591 prescribed amount of thermal load according to economic merit. Indeed, CHP1 is

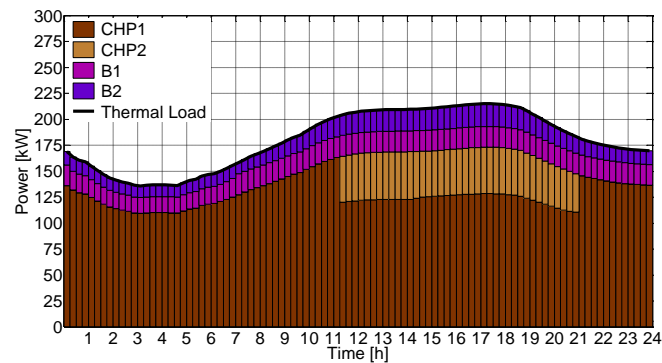
592 working throughout the day and covers 70.3% of thermal demand, and CHP2 is  
 593 exploited only in periods with higher demand, satisfying 9.7%. Furthermore, B1 runs  
 594 close to its rated power covering 10.5% of thermal demand, whereas more expensive B2  
 595 has a daily demand share of 11.0%, most concentrated in peak demand hours.



596

Fig. 8. C2 Strategy: electrical power balance.

597



598

Fig. 9. C2 Strategy: thermal power balance.

599

600

#### 601 **4.2.4. On-Off Operation – C3 Strategy**

602 The C3 strategy is considered by including eq. (27.a)-(27.b) in problem formulation.

603 This simulation set is aimed at investigating the time intervals when the strategy yields

604 the most efficient MG operating condition. This preliminary investigation yielded the

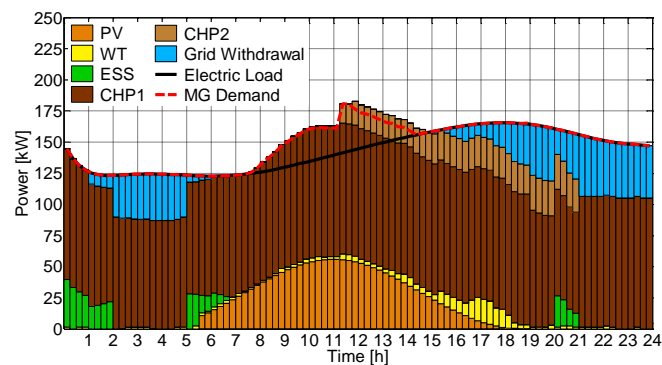
605 activation of C3 strategy in the period from hour 11 to hour 19 for CHP1

606 (  $\beta_{kt}^R = 1 \forall t \in [45, 76]$  ), whereas for CHP2 it is not considered.

607 The electric power balance is depicted in Fig. 10. Due to strategy implementation, CHP  
608 systems cover 76.0% of load. An amount of exchange power at PCC corresponding to  
609 11.2% of load is observed and ESS contribute to 2.8%. Total MG generation exceeds  
610 the imposed load by 4.4%. The production surplus at strategy activation yields an  
611 excess production amounting to 0.6% of the load, that is sold to the distribution  
612 network. Indeed, the remaining 3.8% is dedicated to ESS charge.

613 Thermal power balance in Fig. 11 shows that CHP systems are entrusted to cover 98.1%  
614 of thermal demand (CHP1 covers 86.7% and CHP2 11.4%), whereas boilers are called  
615 to satisfy the residual demand until hour 11, and in the peak hours they are unexploited.  
616 A slight excess of thermal power production is observed in the period of strategy  
617 activation.

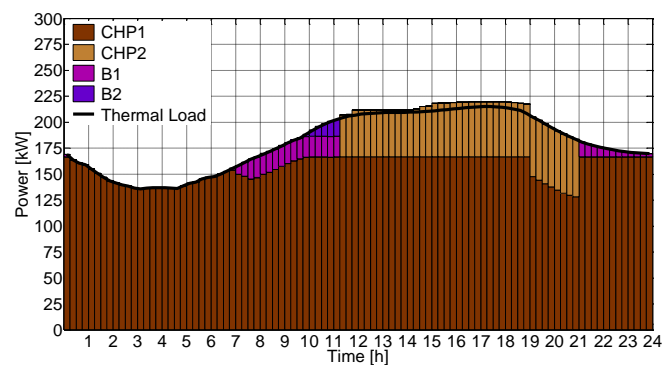
618



619

620

Fig. 10. C3 Strategy: electrical power balance.



621



622 Fig. 11. C3 Strategy: thermal power balance.

623

### 624 4.3. Strategy Comparison and Discussion

625 Technical and economic issues of the implemented strategies in the day-ahead operation  
626 planning of the MG can be compared. In particular, in Table 3 the total daily cost of  
627 each strategy is reported, and the contribution of main cost items is detailed.

628

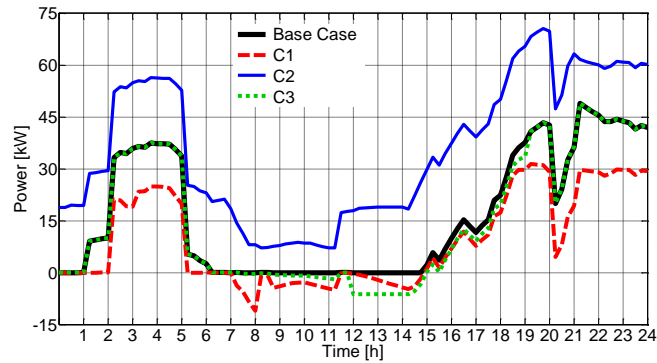
629 Table 3. Daily cost and contributions

Costs \ Strategies	Base Case	C1	C2	C3
Electricity purchase	€ 52.87	€ 33.66	€ 114.16	€ 51.20
CHP fuel cost	€ 440.87	€ 477.17	€ 367.77	€ 448.22
Boiler fuel cost	€ 8.19	€ 3.25	€ 51.96	€ 6.53
Energy selling revenue	€ 0.00	-€ 1.61	€ 0.00	-€ 1.28
Emission cost	€ 4.69	€ 4.99	€ 3.90	€ 4.74
<b>TOTAL COST</b>	<b>€ 506.62</b>	<b>€ 517.46</b>	<b>€ 537.79</b>	<b>€ 509.41</b>

630

631 It can be observed C2 strategy reveals the most expensive, with a maximum difference  
632 of 6% with respect to the Base Case.

633 One of the main factors yielding differences in daily cost is the amount of electricity  
634 exchange at PCC with the distribution network, whose trends, determined as  $P_{Pt} - P_{Dt}$ ,  
635 are shown in Fig. 12. In fact, the highest positive values, i.e. power withdrawal  $P_{Pt}$ , are  
636 reached in C2 strategy and the lowest values are observed in C1 strategy. It can be  
637 pointed out that, in all cases, the electricity withdrawal is reduced when electricity cost  
638 is higher (hours 20-21). Power delivery  $P_{Dt}$  is observed in cases C1 and C3 in central  
639 hours of the day, when the excess comes for free from renewables due to the application  
640 of specific strategy. Whereas, fuel cost is higher in Case C1 due to the more intense  
641 exploitation of the CHP systems.



642

643

Fig. 12. Electricity exchange at PCC with the distribution network in the strategies.

644

645 SOC trends for ESS, in p.u. of total capacity, are illustrated in Fig. 13. It can be noted

646 that SOC at the end of the day returns to initial value, according to the constraint (3.b).

647 This behavior contributes to extend ESS life as well, since it depends on the number of

648 charge/discharge cycles [27].

649 ESS has the task of storing excess energy, especially in hours 9-13 when RES

650 production is high and the electricity price is generally low. This yields an increase of

651 total MG demand, and limits power injection into the network. In fact, storing energy in

652 excess production periods and using it, even considering non-ideal efficiencies, to cover

653 the demand in peak price periods (hours 20-21), reveals in general more convenient than

654 selling excess production and buying energy in peak price hours. Moreover, the ESS is

655 discharged until hour 6, covering part of the load demand and avoiding network

656 withdrawal, in order to be ready to charge in the presence of excess power.

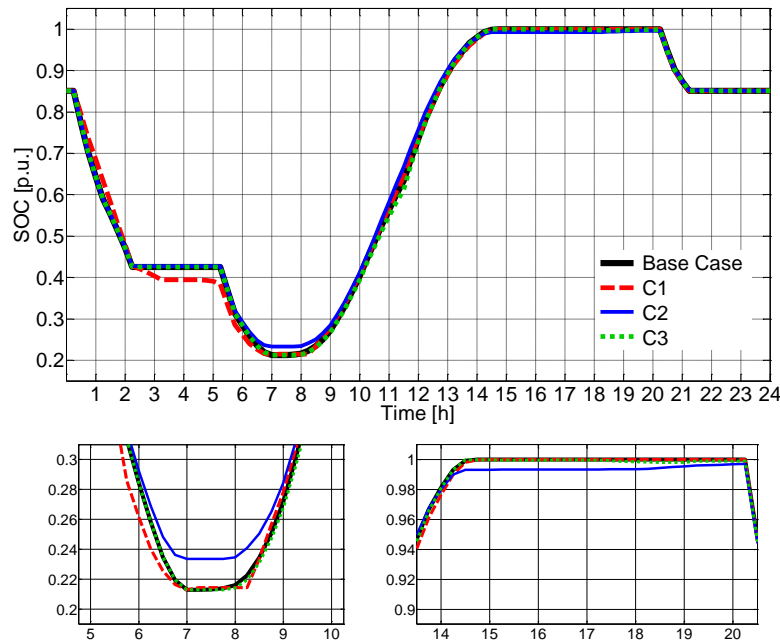
657 Correspondently, minimum SOC of 30 kWh (0.21 p.u.) is observed in C3, along with

658 maximum daily energy of 94.4 kWh. Slight differences are observed with respect to

659 Base Case in C1, with deeper discharge in hour 3. Minimum exploitation of ESS is

660 observed in C2 with daily energy supply of 91.5 kWh, and those differences are

661 highlighted in the details at bottom of Fig. 13.



662

663

Fig. 13. SOC of ESS in the strategies.

664

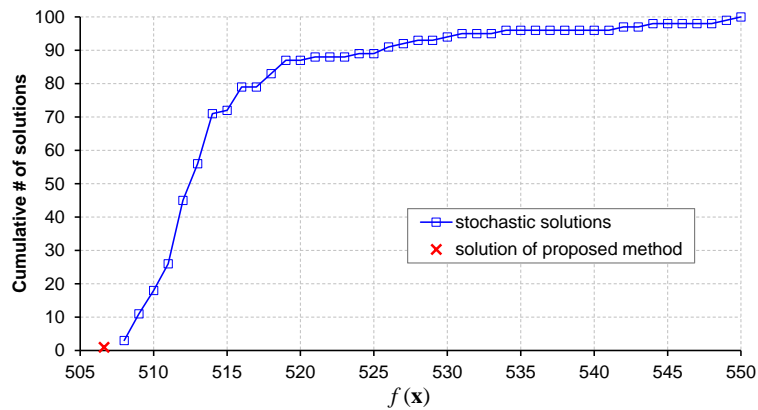
665 It can be observed that in Base Case and C2 the thermal demand is strictly satisfied  
 666 during the day, i.e. constraint (24) reduces to an equality, whereas the excess thermal  
 667 power is due only to CHP strategies. Being less efficient, boilers are usually called to  
 668 compensate for peak load, and B2 reveals the less preferable. In addition, in C1 and C3  
 669 Strategies the CHP systems reach a global average efficiency, given by the sum of  
 670 electrical and thermal efficiencies, higher than 75%. This threshold often characterizes  
 671 cogeneration systems with high-efficiency.

672 As regards emissions, their contribution range from 0.75% to 1.0% of total daily cost. In  
 673 particular, C1 strategy shows higher emissions (1,241 kg of CO<sub>2</sub> in a day), whereas C2  
 674 reveals the less pollutant one (971 kg of CO<sub>2</sub> in a day). However, it can be seen that  
 675 higher emissions are not related to higher total cost.

676 In CHP operation programs resulting from the procedure, it is observed that production

677 level does not fall below experimental minimum amount (1 kW), since the  
678 corresponding low efficiency, and consequent high cost, makes it inconvenient to use  
679 CHP below 1 kW with respect to other sources. This allows to achieve analogous results  
680 with respect to other approaches introducing integer decision variables [24][64].

681 In order to validate the optimality of the achieved solution, obtained by the NLP  
682 formulation solved through SQP starting from the solution of the linearized problem, a  
683 set of further 100 starting points satisfying the constraints of the linearized problem is  
684 exploited [65]. These starting points are generated by stochastic variations of the  
685 linearized problem solution, according to normal distributions with zero mean and 20%  
686 as confidence interval for each state variable. The problem is therefore solved through  
687 SQP by using each of these starting points, and the obtained results for the Base Case  
688 are reported in Fig. 14, where their cumulative distribution is compared with the  
689 solution of the proposed method. It can be seen that the solution obtained by means of  
690 the method described in Section 4.1 is the lowest, and most of solutions with stochastic  
691 starting points are close, but not better. Analogous results are obtained for the other  
692 three cases. Therefore, these results confirm that the overall proposed procedure for  
693 NLP problem solution, where the starting point is the solution of the linearized problem,  
694 reasonably guarantees the achievement of the optimal solution.



695

696

Fig. 14. Comparison of solutions with different starting points in the Base Case.

697

## 698 5. Conclusions

699 In this paper, an optimization procedure for the day-ahead operational scheduling of a

700 MG has been proposed. A non-linear programming problem is formulated, accounting

701 for actual features of DG technologies and for different energy pricing schemes. Electric

702 and thermal generation systems, along with CHP devices, have been modeled and the

703 operation of ESS has been taken into account, in order to minimize operational costs on

704 a daily horizon while satisfying electric and thermal load. Moreover, different strategies

705 have been exploited according to operating modes of CHP systems. These strategies

706 have been tested by implementing case studies on an experimental MG and comparing

707 technical and economic outcomes. Simulation results have proved that the different

708 strategies remarkably affect operation costs, reaching significant reduction of primary

709 energy consumption and pollutant emissions. Strategy effectiveness depends on MG

710 structure and particular condition of the considered day. The proposed approach is

711 flexible enough to incorporate other types of DG units.

712 Future work will deal with the inclusion of thermal storage, the simulation of periods

713 with different connection modes (islanded or grid-connected), and the implementation

714 of the second-stage procedure to cope with deviations of renewable production and load  
715 from the predicted levels in the real time. Finally, the application in actual  
716 SCADA/EMS system for MG management is envisaged, as exemplified in [66] for a  
717 different configuration.

718

## 719 **References**

- 720 [1] D. E. Olivares, A. Mehrizi-Sani, A. H. Etemadi, C. A. Canizares, R. Iravani, M. Kazerani, A.  
721 H. Hajimiragha, O. Gomis-Bellmunt, M. Saeedifard, R. Palma-Behnke, G. A. Jimenez-Estevez,  
722 N. D. Hatziargyriou, “Trends in microgrid control,” *IEEE Trans. Smart Grid*, vol. 5, no. 4, pp.  
723 1905–1919, Jul. 2014. <http://dx.doi.org/10.1109/TSG.2013.2295514> .
- 724 [2] C. Chowdhury, S.P. Chowdhury, P. Crossley, *Microgrids and Active Distribution Networks*.  
725 London, UK: IET, 2009. <http://dx.doi.org/10.1049/PBRN006E> .
- 726 [3] C. Natesan, S.K. Ajithan, S. Chozhavendhan, A. Devendhiran, “Power Management Strategies  
727 in Microgrid: A Survey”, *International Journal of Renewable Energy Research*, Vol. 5 No. 2,  
728 pp. 1-7, 2015.
- 729 [4] Z. Bao, Q. Zhou, Z. Yang, Q. Yang, L. Xu, T. Wu, “A Multi Time-Scale and Multi Energy-  
730 Type Coordinated Microgrid Scheduling Solution—Part I: Model and Methodology”, *IEEE*  
731 *Transactions on Power Systems*, vol. 30, No. 5, pp. 2257-2266, Sept. 2015,  
732 <http://dx.doi.org/10.1109/TPWRS.2014.2367127> .
- 733 [5] A. A. Khan, M. Naeem, M. Iqbal, S. Qaisar, A. Anpalagan, “A compendium of optimization  
734 objectives, constraints, tools and algorithms for energy management in microgrids”, *Renewable*  
735 *and Sustainable Energy Reviews* vol. 58, pp. 1164-1683, 2016,  
736 <http://dx.doi.org/10.1016/j.rser.2015.12.259> .
- 737 [6] H. Daneshi, H. Khorashadi-Zadeh, “Microgrid Energy Management System: A Study of  
738 Reliability and Economic Issues”, ” in *Proc. IEEE Power Energy Soc. Gen. Meeting*, San  
739 Diego, CA, 2012, pp. 1–5. <http://dx.doi.org/10.1109/PESGM.2012.6344957> .

- 740 [7] J. Chen, X. Yang, L. Zhu, M. Zhang, “Microgrid Economic Operation and Research on  
741 Dispatch Strategy”, In *Proc. Power Engineering and Automation Conference (PEAM)*, Wuhan,  
742 2012 pp. 1-6. <http://dx.doi.org/10.1109/PEAM.2012.6612416> .
- 743 [8] G.-C. Liao, “The Optimal Economic Dispatch of Smart Microgrid Including Distributed  
744 Generation”, In *Proc. IEEE 2nd Int. Symp. on Next-Generation Electronics (ISNE)*, Kaohsiung,  
745 2013, pp. 473-477. <http://dx.doi.org/10.1109/ISNE.2013.6512401> .
- 746 [9] A. Chaouachi, R.M. Kamel, R. Andoulsi, K. Nagasaka, “Multiobjective Intelligent Energy  
747 Management for a Microgrid”, *IEEE Trans. Ind. Electron.*, vol. 60, no. 4, pp. 1688–1699, Apr.  
748 2013. <http://dx.doi.org/10.1109/TIE.2012.2188873> .
- 749 [10] R. Palma-Behnke, C. Benavides, F. Lanas, B. Severino, L. Reyes, J. Llanos, D. Saez, “A  
750 Microgrid Energy Management System Based on the Rolling Horizon Strategy”, *IEEE Trans.*  
751 *Smart Grid*, vol. 4, no. 2, pp. 996–1006, Jun. 2013.  
752 <http://dx.doi.org/10.1109/TSG.2012.2231440>
- 753 [11] Q. Jiang, M. Xue, G. Geng, “Energy Management of Microgrid in Grid-Connected and Stand-  
754 Alone Modes”, *IEEE Trans. Power Syst.*, vol. 28, no. 3, pp.3380 -3389, Aug. 2013.  
755 <http://dx.doi.org/10.1109/TPWRS.2013.2244104> .
- 756 [12] M. Strelec, J. Berka, “Microgrid Energy Management based on Approximate Dynamic  
757 Programming”, in *Proc. 4th IEEE/PES ISGT Europe*, Copenhagen, Denmark, 2013, pp. 1-5.  
758 <http://dx.doi.org/10.1109/ISGTEurope.2013.6695439> .
- 759 [13] M. Mahmoodi, P. Shamsi, B. Fahimi, “Optimal Scheduling of Microgrid Operation  
760 Considering the Time-of-Use Price of Electricity”, Industrial Electronics Society, IECON 2013,  
761 Vienna, 2013, Pages 2127-2132. <http://dx.doi.org/10.1109/IECON.2013.6699460> .
- 762 [14] D. Zhang, S. Li, P. Zeng, C. Zang, “Optimal Microgrid Control and Power Flow Study With  
763 Different Bidding Policies by Using PowerWorld Simulator”, *IEEE Trans. Sustain. Energy*,  
764 vol. 5, no. 1, pp. 282-292, Oct. 2014. <http://dx.doi.org/10.1109/TSTE.2013.2281811>

- 765 [15] M. Ross, C. Abbey, F. Bouffard, G. Joos, “Multiobjective Optimization Dispatch for  
766 Microgrids With a High Penetration of Renewable Generation”, *IEEE Trans. Sustain. Energy*,  
767 vol. 6, no. 4, pp. 1306-1314, Oct. 2015. <http://dx.doi.org/10.1109/TSTE.2015.2428676> .
- 768 [16] V. Prema, K. Uma Rao, “Predictive Models For a Power Management Of a Hybrid Microgrid-  
769 A Review”, in *Proc. Int. Conf. Advances in Energy Conversion Technologies (ICAECT)*,  
770 Manipal, 2014, pp. 7-12. <http://dx.doi.org/10.1109/ICAECT.2014.6757053> .
- 771 [17] I. Prodan, E. Zio, “An optimization-based control approach for reliable microgrid energy  
772 management under uncertainties”, in *Proc. IEEE ISEPS Workshop*, Bucharest, 2013, pp. 4-7.  
773 <http://dx.doi.org/10.1109/ISEPS.2013.6707950> .
- 774 [18] R. A. Gupta, N. K. Gupta, “A robust optimization based approach for microgrid operation in  
775 deregulated environment”, *Energy Conversion and Management*, vol. 93, pp. 131-131, 2015,  
776 <http://dx.doi.org/10.1016/j.enconman.2015.01.008> .
- 777 [19] S. A. Alavi, A. Ahmadian, M. Aliakbar-Golkar, “Optimal probabilistic energy management in a  
778 typical micro-grid based-on robust optimization and point estimate method”, *Energy  
779 Conversion and Management*, vol. 95, pp. 314-325, 2015,  
780 <http://dx.doi.org/10.1016/j.enconman.2015.02.042> .
- 781 [20] C. Marnay, G. Venkataramanan, G. Stadler, A. Siddiqui, R. Firestone, R. Chandran “Optimal  
782 technology selection and operation of microgrids in commercial buildings”, *IEEE Trans Power  
783 Syst.* Vol. 23, no. 3, pp. 975-982, 2008, <http://dx.doi.org/10.1109/TPWRS.2008.922654> .
- 784 [21] M. Motevasel, A. R. Seifi, T. Nikham, “Multi-objective Energy management of CHP  
785 (combined heat and power)-based micro-grid”, *Energy*, vol. 51, pp. 123-136, 2013,  
786 <http://dx.doi.org/10.1016/j.energy.2012.11.035> .
- 787 [22] G. Bruni, S. Cordiner, V. Mulone, V. Rocco, F. Spagnolo, “A study on the Energy management  
788 in domestic micro-grids based on Model Predictive Control Strategies”, *Energy Conversion and  
789 Management*, vol. 102, pp. 50-58, 2015, <http://dx.doi.org/10.1016/j.enconman.2015.01.067> .



- 790 [23] X. Lin, P. Li, J. Ma, Y. Tian, D. Su, “Dynamic Optimal Dispatch of Combined Heating and  
791 Power Microgrid Based on Leapfrog Firefly Algorithm”, Proc. of 2015 IEEE 12th Int. Conf. on  
792 Networking, Sensing and Control, Taipei, Taiwan April 9-11, 2015, pp. 416-420.
- 793 [24] M. Alipour, B. Mohammadi-Ivatloo, “Stochastic Scheduling of Renewable and CHP-Based  
794 Microgrids”, IEEE Trans. Industrial Informatics, vol. 11, no. 5, pp. 1049-1058, October 2015,  
795 <http://dx.doi.org/10.1109/TII.2015.2462296> .
- 796 [25] K. Basu, A. Bhattacharya, S. Chowdhury, S.P. Chowdhury, “Planned Scheduling for Economic  
797 Power Sharing in a CHP-Based Micro-Grid”, IEEE Trans. Power Systems, vol. 27, no. 1, pp.  
798 30-38, February 2012, <http://dx.doi.org/10.1109/TPWRS.2011.2162754> .
- 799 [26] X. Jin, H. Li, T. Jin, X. Xu, M. Wang, J., Meng, “Economical and Coordinated Dispatch of  
800 CHP Based Microgrid with Renewable Energy Resources”, Advanced Materials Research  
801 Vols. 960-961, pp. 1022-1028, 2014 [http://dx.doi.org/10.4028/www.scientific.net/AMR.960-](http://dx.doi.org/10.4028/www.scientific.net/AMR.960-961.1022)  
802 [961.1022](http://dx.doi.org/10.4028/www.scientific.net/AMR.960-961.1022)
- 803 [27] L. Majic, I. Krzelj, M. Delimar, “Optimal scheduling of a CHP system with energy storage”,  
804 Proc. of MIPRO 2013, May 20-24, 2013, Opatija, Croatia, pp. 1253-1257.
- 805 [28] D. Zhang, S. Evangelisti, P. Lettieri, L.G. Papageorgiou, “Economic and environmental  
806 scheduling of smart homes with microgrid: DER operation and electrical tasks”, Energy  
807 Conversion and Management, vol. 110, pp. 113-124, 2016,  
808 <http://dx.doi.org/10.1016/j.enconman.2015.11.056>
- 809 [29] K.C. Kavvadias, A.P. Tosios, Z.B. Maroulis, “Design of a combined heating, cooling and  
810 power system: Sizing, operation strategy selection and parametric analysis”, *Energy Convers.*  
811 *and Managem.*, vol. 51, pp. 833-845, 2010, <http://dx.doi.org/10.1016/j.enconman.2009.11.019>
- 812 [30] E. Carpaneto, G. Chicco, P. Mancarella, A. Russo, “Cogeneration planning under uncertainty-  
813 Part I: Multiple time frame approach”, *Appl. Energy*, vol. 88, no. 4, pp. 1075-1083, 2011.  
814 <http://dx.doi.org/10.1016/j.apenergy.2010.10.014> .

- 815 [31] E. Perea, N. Ruiz, I. Cobelo, Z. Lizuain, A. Carrascal, “A novel optimization algorithm for  
816 efficient economic dispatch of Combined Heat and Power devices”, *Energy and Buildings*, vol.  
817 111, pp. 207-514, January 2016. <http://dx.doi.org/10.1016/j.enbuild.2015.11.025>
- 818 [32]H. Bowen. Z. Zhanghua, “Stochastic Multi-objective Dynamic Optimal Dispatch for Combined  
819 Heat and Power Microgrid”, *Proc. of 2016 IEEE PES Asia-Pacific Power and Energy*  
820 *Conference (APPEEC) – Xi’an, China, 25-28 October 2016*, pp. 2369-2373,  
821 <http://dx.doi.org/10.1109/APPEEC.2016.7779908>
- 822 [33] M. Barbarić, D. Lončar, “Energy management strategies for combined heat and electric power  
823 micro-grid”, *Thermal Science*, vol. 20, no. 4, pp. 1091-1103, 2016.  
824 <http://dx.doi.org/10.2298/TSCI151215081B> .
- 825 [34] L. Ma, N. Liu, J. Zhang, W. Tushar, C. Yuen, “Energy Management for Joint Operation of  
826 CHP and PV Prosumers Inside a Grid-Connected Microgrid: A Game Theoretic Approach”,  
827 *IEEE Trans. Industrial Informatics*, vol. 12, no. 5, pp. 1930-1942, October 2016.  
828 <http://dx.doi.org/10.1109/TII.2016.2578184> .
- 829 [35] T. Schittekatte, M. Stadler, G. Cardoso, S. Mashayekh, N. Sankar, “The impact of short-term  
830 stochastic variability in solar irradiance on optimal microgrid design”, *IEEE Transactions on*  
831 *Smart Grid*, accepted 2016 <http://dx.doi.org/10.1109/TSG.2016.2596709> .
- 832 [36] M.J. Sanjari, H. Karami, H.B. Gooi, “Micro-generation dispatch in a smart residential multi-  
833 carrier energy system considering demand forecast error”, *Energy Conv. and Manag.* vol. 120,  
834 pp. 90-99, July 2016. <http://dx.doi.org/10.1016/j.enconman.2016.04.092> .
- 835 [37] J. Aghaei, M.-I. Alizadeh, “Multi-objective self-scheduling of CHP (Combined heat and  
836 power)-based microgrids considering demand response programs and ESSs (energy storage  
837 systems)”, *Energy*, vol. 55, pp. 1044-1054, June 2013.  
838 <http://dx.doi.org/10.1016/j.energy.2013.04.048> .
- 839 [38] M. Restepo, C. A. Canizares, M. Kazerani, “Three-Stage Distribution Feeder Control  
840 Considering Four-Quadrant EV Chargers”, *IEEE Transactions on Smart Grid*, Accepted  
841 December 2016, <http://dx.doi.org/10.1109/TSG.2016.2640202> .

- 842 [39] S. S. Soman, H. Zareipour, O. Malik, P. Mandal, “A review of wind power and speed  
843 forecasting methods with different time horizons”, in *Proc. North Amer. Power Symp. (NAPS)*,  
844 Arlington, 2010, pp.1-8. <http://dx.doi.org/10.1109/NAPS.2010.5619586> .
- 845 [40] J. A. Duffie, W. A. Beckman, *Solar Engineering of Thermal Processes*. Fourth Edition , John  
846 Wiley & Sons, Inc., Hoboken, NJ, USA.2013.. <http://dx.doi.org/10.1002/9781118671603>
- 847 [41] E. Skoplaki, A.G. Boudouvis, J.A. Palyvos, “A simple correlation for the operating temperature  
848 of photovoltaic modules of arbitrary mounting”, *Solar Energy Mater. Solar Cells*, vol. 92, no.  
849 11, pp.1393-1402, 2008. <http://dx.doi.org/10.1016/j.solmat.2008.05.016> .
- 850 [42] J. Shi, W.-J. Lee, Y. Liu, Y. Yang, P. Wang, “Forecasting Power Output of Photovoltaic  
851 Systems Based on Weather Classification and Support Vector Machines”, *IEEE Trans. Ind.*  
852 *Appl.*, vol. 48, no. 3, pp. 1064-1069, May/June 2012:  
853 <http://dx.doi.org/10.1109/TIA.2012.2190816> .
- 854 [43] O. H. Mohammed, Y. Amirat, M. Benbouzid, T. Tang, “Hybrid Generation Systems Planning  
855 Expansion Forecast: A critical State of the art review”, *Proc. of 39<sup>th</sup> IECON IEEE IES Annual*  
856 *Conference*, Vienna, 2013, pp. 1668-1673: <http://dx.doi.org/10.1109/IECON.2013.6699383> .
- 857 [44] L. H. Macedo, J. F. Franco, M. J. Rider, R. Romero, “Optimal Operation of Distribution  
858 Networks Considering Energy Storage Devices”, *IEEE Trans. Smart Grid*, vol. 6 no. 6, Nov.  
859 2015, pp. 2825-2836: <http://dx.doi.org/10.1109/TSG.2015.2419134> .
- 860 [45] B. Zhao, X. Zhang, J. Chan, C. Wang, L. Guo, “Operation Optimization of Standalone  
861 Microgrids Considering Lifetime Characteristics of Battery Energy Storage System”, *IEEE*  
862 *Trans. Sust. Energy*, vol. 4, no., 4, pp. 934-943, October 2013.  
863 <http://dx.doi.org/10.1109/TSTE.2013.2248400>
- 864 [46] M. Gitizadeh, H. Fakhrazadegan, “Battery capacity determination with respect to optimized  
865 energy dispatch schedule in grid-connected photovoltaic (PV) systems”, *Energy*, vol. 65, pp.  
866 665-674, February 2014. <http://dx.doi.org/10.106/j.energy.2013.12.018>

- 867 [47] E. Hittinger, T. Wiley, J. Kluza, J. Whitacre, “Evaluating the value of batteries in microgrid  
868 electricity systems using an improved Energy Systems Model”, *Energy Conv. and Manag.*, vol.  
869 89, pp. 458-472, January 2015. <http://dx.doi.org/10.1016/j.enconman.2014.10.011>
- 870 [48] A.F. Orlando, M.M. Huamaní, L. DoVala, J.V. Araujo, “A methodology for evaluating field  
871 performance and emissions of a gas microturbine based cogeneration system”, *Engenharia*  
872 *Térmica*, vol. 7, n. 1, pp.21-30, 2008.
- 873 [49] H. Kanchev, F. Colas, V. Lazarov, B. Francois, “Emission reduction and economical  
874 optimization of an urban microgrid operation including dispatched PV-based active  
875 generators”, *IEEE Transactions On Sustainable Energy*, vol. 5, no. 4, pp. 1397-1405, Oct.  
876 2014. <http://dx.doi.org/10.1109/TSTE.2014.2331712> .
- 877 [50] A. Rosato, S. Sibilio, “Calibration and validation of a model for simulating thermal and electric  
878 performance of an internal combustion engine-based micro-cogeneration device”, *Applied*  
879 *Thermal Engineering*, vol. 45-46, pp. 79-98, Dec. 2012.  
880 <http://dx.doi.org/10.1016/j.applthermaleng.2012.04.020>
- 881 [51] N. Badea, *Design for Micro-Combined Cooling, Heating and Power Systems*. London:  
882 Springer, 2015. <http://dx.doi.org/10.1007/978-1-4471-6254-4>
- 883 [52] Deliberazione AEEG 493/2012/R/efr “Approvazione delle modalità per l’attribuzione dei  
884 corrispettivi di sbilanciamento e dei corrispettivi a copertura dei costi amministrativi da  
885 attribuire ai produttori in regime di ritiro dedicato e di tariffa fissa onnicomprensiva”, 22  
886 November 2012 (in Italian).
- 887 [53] A. Cagnano, E. De Tuglie, M. Dicorato, G. Forte, M. Trovato, “PrInCE Lab experimental  
888 microgrid – Planning and operation issues”, *Proc. of 2015 IEEE 15<sup>th</sup> EEEIC Int. Conf.*, Rome,  
889 Italy, pp. 1671-1676, <http://dx.doi.org/10.1109/EEEIC.2015.7165423> .
- 890 [54] B. Aluisio, A. Cagnano, E. De Tuglie, M. Dicorato, G. Forte, M. Trovato, “An architecture for  
891 the monitoring of microgrid operation”, *Proc. of 2016 IEEE EESMS Conference*, Bari, Italy,  
892 pp. 1-6, <http://dx.doi.org/10.1109/EESMS.2016.7504809> .
- 893 [55] <http://www.wunderground.com/>

- 894 [56] <http://www.amgasbarisrl.it/> (in Italian)
- 895 [57] <http://www.sendeco2.com> .
- 896 [58] A. Bhatt, A. Shrivastava, M. Pandit, H. M. Dubey, “Dynamic Scheduling of Operating Energy  
897 and Reserve in Electricity Market with Ramp Rate Constraints”, in *Proc. IEEE IET CRAIE-*  
898 *2014 Conf.*, Jaipur, India, May 2014, pp. 1-6. <http://dx.doi.org/10.1109/ICRAIE.2014.6909313>
- 899 [59] F. A. Bayer, G. Notarstefano, F. Allgower, “A Projected SQP method for Nonlinear Optimal  
900 Control with Quadratic Convergence”, *Proc. of 52nd IEEE Conference on Decision and*  
901 *Control*, December 10-13, 2013, Florence, Italy, pp. 6463-6468,  
902 <http://dx.doi.org/10.1109/CDC.2013.6760912>
- 903 [60] P. E. Gill., E. Wong, “Sequential quadratic programming methods”, in: J. Lee, S. Leyffer,  
904 “Mixed Integer Nonlinear Programming”, Vol. 147 of The IMA Volumes in Mathematics its  
905 Applications, Springer Science, 2012, pp. 147-224, [http://dx.doi.org/10.1007/978-1-4614-](http://dx.doi.org/10.1007/978-1-4614-1927-3_6)  
906 [1927-3\\_6](http://dx.doi.org/10.1007/978-1-4614-1927-3_6)
- 907 [61] J. Nocedal, S. J. Wright, “Numerical Optimization – Second Edition”. Springer Series in  
908 Operations Research, Springer Verlag, 2006.
- 909 [62] A. D. Belegundu, T. R. Chandrupatla, “Optimization Concepts and Applications in Engineering  
910 – Second Edition”, Cambridge University Press, 2011.
- 911 [63] D. P. Bertsekas, “Nonlinear Programming: 3rd Edition”, Athena Scientific, 2016.
- 912 [64] I. G. Moghaddam, M. Saniei, E. Mashhour, “A comprehensive model for self-scheduling an  
913 energy hub to supply cooling, heating and electrical demands of a building”, *Energy*, vol. 94,  
914 pp. 157-170, January 2016. <http://dx.doi.org/10.1016/j.energy.2015.10.137>
- 915 [65] R. Fourer, D. M. Gay, B. W. Kernighan, “AMPL: A Modeling Language for Mathematical  
916 Programming – Second Edition”, Duxbury Press / Brooks / Cole Publishing Company, 2003.
- 917 [66] B. Aluisio, A. Cagnano, E. De Tuglie, M. Dicorato, G. Forte, M. Trovato, “PrInCE lab  
918 microgrid: Early experimental results”, *2016 AEIT International Annual Conference (AEIT)*,  
919 Capri (Italy), 5-7 Oct. 2016, pp. 1-6, <http://dx.doi.org/10.23919/AEIT.2016.7892770>
- 920